CONF-840408--16
BNL-NUREG-34824

TWIST: A TRANSIENT TWO-DIMENSIONAL INTRA-SUBASSEMBLY THERMAL HYDRAULICS MODEL FOR LMFBRs*

BNL-NUREG--34824
DE84 014383

Mohsen Khatib-Rahbar and Erik G. Cazzoli
Brookhaven National Laboratory
Department of Nuclear Energy
Upton, New York 11973
(516) 282-2626

ABSTRACT

Mathematical models and numerical methods for a two-dimensional porous body simulation of steady state and transient thermal-hydraulics conditions in LMFBR subassemblies resulting in the TWIST computer code are presented. Comparison of calculated results to steady state and transient out-of-pile sodium experiments show good agreement for cross-assembly temperature distributions for a wide range of heat transfer and flow conditions.

INTRODUCTION

In Liquid Metal Fast Breeder Reactor (LMFBR) core designs, the fuel, blanket, control and shield assemblies are packed in a hexagonal configuration.

The fuel and blanket assemblies consist of cylindrical fuel pins arranged in a closely packed triangular array separated by helical wire wraps. These wires also induce swirling flow which provide coolant mixing between subchannels.

During full power, steady state operation, the sodium flow Reynolds numbers range from 1.5×10^4 in the radial blanket to about 10^5 in the fuel assemblies. Following protected loss-of-flow transients, the flow regime changes from turbulent to transition and finally laminar as the Reynolds numbers are reduced; subsequently leading to changes in the associated heat transfer modes from forced to mixed and eventually free convection.[1,2]

A number of detailed computer codes, generally written for applications to LMFBR design, are available.[3-7] Due to the physical and numerical sophistication of these models, their application to long duration transient safety analysis problems is often constrained. Therefore, it is desirable to develop a numerically efficient model supported by experimental data capable of predicting heat transfer and flow regime behavior in LMFBR subassemblies during protected loss-of-flow transients.

*Work sponsored by the U.S. Nuclear Regulatory Commission and in part by the Power Nuclear and Fuel Development Corporation (PNC) of Japan.

The purpose of the present paper is to formulate a simple, transient two-dimensional thermal-hydraulics model, supported by experimental data, resulting in TWIST (TWo-dimensional Intra-Subassembly Thermal-hydraulics) computer code, for study of steady state and transient forced, mixed and free convection conditions in LMFBR subassemblies.

MATHEMATICAL MODEL

In the porous-body treatment, the presence of fuel rods is taken into account by inclusion of a volume porosity in the governing equations. The energy generation by the rods is modeled by a continuous volumetric heat source distribution.[8] The energy transfer in the transverse direction is modeled by molecular conduction and an empirically determined effective eddy diffusivity.

For simplicity, the rod bundle will be approximated by a two-dimensional porous slab of width ℓ corresponding to the assembly flat-to-flat for which the following assumptions apply:

(1) two-dimensional, incompressible flow,
(2) negligible axial conduction,
(3) negligible viscous dissipation,
(4) Boussinesq approximation is valid, and
(5) uniform pressure at any axial level.

Therefore, the conservation of mass, energy and axial momentum equations can be written as follows:[9]

(a) Conservation of Mass:

$$\frac{\partial(\rho u)}{\partial x} + \frac{\partial(\rho v)}{\partial y} = 0 \qquad (1)$$

(b) Conservation of Energy:

$$\frac{\partial T}{\partial t} + u\frac{\partial T}{\partial x} + v\frac{\partial T}{\partial y} = \alpha_e \frac{\partial^2 T}{\partial y^2} + \frac{Q'''(x,y)}{\rho c_p} \qquad (2)$$

MASTER

NOTICE

PORTIONS OF THIS REPORT ARE ILLEGIBLE. It has been reproduced from the best available copy to permit the broadest possible availability.

DISTRIBUTION OF THIS DOCUMENT IS UNLIMITED

(c) Conservation of Axial Momentum:

$$\frac{\partial u}{\partial t} + u\frac{\partial u}{\partial x} + v\frac{\partial u}{\partial y} = -\frac{1}{\rho}\frac{\partial P}{\partial x} - g\frac{\rho^*}{\rho}[1-\beta(T-T^*)] + \nu\frac{\partial^2 u}{\partial y^2} + \frac{f}{2D_e\lambda^2}u^2 \quad (3)$$

and

$$f = f(Re)$$

Subject to the following initial and boundary conditions:

Initial Conditions

$$\left.\begin{array}{l} u(x,y,o) \\ v(x,y,o) \\ T(x,y,o) \end{array}\right\} \text{ known (Through Steady-State Solution)} \quad (4)$$

Boundary Conditions

$$\begin{array}{lll} u = v = o & & \text{at duct walls} \\ u(o,y,t) & = & \text{specified} \\ v(o,y,t) & = & o \\ T(o,y,t) & = & T^* \text{ (specified)} \\ Q'''(x,y,t) & = & \text{specified} \end{array} \quad (5)$$

where ρ is the fluid density, u is the superficial velocity in the longitudinal direction, v is the superficial velocity in the transverse direction, T is the fluid temperature, Q''' is the volumetric heat generation rate, ν is the kinematic viscosity, P is the pressure, g is the gravitational acceleration, β is the volumetric thermal expansion coefficient, D_e is the hydraulic equivalent diameter, f is the friction factor, λ is the axial area fraction occupied by the coolant (porosity), c_p is the heat capacity at constant pressure, and α_e is the effective thermal diffusivity defined as:

$$\alpha_e = k_e/\rho c_p = \varepsilon_h + \kappa k/\rho c_p \quad (6)$$

where the eddy diffusivity of heat, ε_h (m^2/s) is defined by

$$\varepsilon_h = \hat{u} D_e \varepsilon^* \quad (7)$$

Here $\hat{u}$ is the average velocity, and ε^* is the mixing parameter empirically determined.[9]

The shape factor κ (also known as tortuosity) for molecular conductivity k is to account for the reduction in thermal conduction due to the presence of the fuel rods inside the sodium and is assumed to be given by,

$$\kappa = \frac{\lambda}{1 + 0.5(1-\lambda)} \quad (8)$$

It must be noted that, the transverse momentum equation need not be formulated since the pressure is assumed to be uniform in the transverse direction.

The energy equations for the duct wall structure and the interstitial sodium region adjacent to the duct wall can be written as:

Duct Wall

$$M_w C_w \frac{\partial T_w}{\partial t} = \frac{k_w}{\delta_w} A_w (T_s - T_w) + k_s\left(\frac{\partial T}{\partial y}\right)_w \quad (9)$$

Interstitial Sodium

$$M_s C_s \frac{\partial T_s}{\partial t} = \frac{k_w}{\delta_w} A_w (T_w - T_s) \quad (10)$$

Where M is the mass, C is the specific heat, A is the duct wall outside area, δ is the duct thickness, and the subscripts w and s refer to the duct wall and interstitial sodium, respectively.

At steady state, the subassembly is assumed to be adiabatic, and therefore;

$$\left(\frac{\partial T}{\partial y}\right)_w = 0; \quad T_s = T_w \quad (11)$$

METHOD OF SOLUTION

Finite Difference Equations

The conservation equation of the previous section are of parabolic nature; that is, convection in the axial direction dominates the axial diffusion. It is this feature that imports the one-way character to the streamwise direction. Obviously, no reverse flow in the axial direction would be acceptable.

Equations (1), (2), (3), (9), and (10) are expressed in a fully implicit finite difference form.[9] Fig. 1 shows the schematics of the coordinate system for the finite difference equations and their associated grid structure.

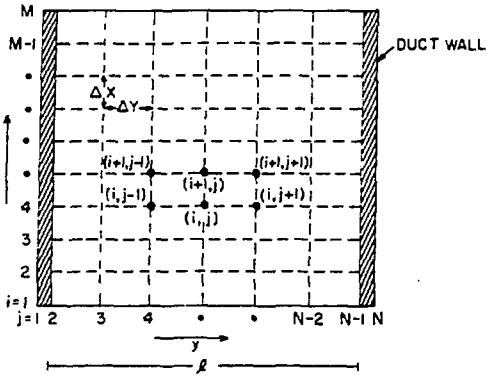

Figure 1 Coordinate System for the Finite Difference Equations

The finite difference form of the coolant and duct wall structure energy equations are transformed to the following form:

$$\bar{\bar{A}} \cdot \bar{T}^{k+1} = \bar{B} \qquad (12)$$

Where, the tridiagonal matrix, $\bar{\bar{A}}$ is a function of the advanced time upstream velocities, $\bar{B}$ is the vector of the right-hand sides,[9] and $\bar{T}^{k+1}$ is the vector of the advanced-time temperatures $(T_{i+1,1}, T_{i+1,2}, \ldots, T_{i+1,N})^{k+1}$.

Similarly, the axial momentum and mass continuity difference equations are also transformed into the following form:

$$\bar{\bar{C}}\, \bar{X}^{k+1} = \bar{D} \qquad (13)$$

Here, $\bar{\bar{C}}$ and $\bar{D}$ are the coefficient matrix and the vector of the right-hand sides, respectively, and are given in [9] and $\bar{X}^{k+1}$ is the vector of the advanced time velocities and the pressure gradient namely,

$$\bar{X}^{k+1} = [u_{i+1,3}, u_{i+1,4}, \ldots, u_{i+1,N-2}; \Delta P_{i+1}]^{k+1} \qquad (14)$$

It is important to note that $\bar{D}$ is dependent upon the $\bar{T}^{k+1}$ values.

Numerical Solution Technique

The steady state and transient solution techniques follow the same procedure, except for steady state calculations the time derivations are set to zero ($\frac{\partial}{\partial t}=0$). The numerical solution procedure is as follows:

(1) Start at i=1 row; and solve Eq. (12) for $T_{2,1}$, $T_{2,2}$, ..., $T_{2,N}$ using the Gaussian elimination technique.

(2) Calculate the physical properties as a function of $T_{2,j}$'s.

(3) Solve Eq. (13) for $u_{2,3}$, $u_{2,4}$, ..., $u_{2,N-2}$ and ΔP_2 using the Gauss-Jordan reduction method.

(4) Now, back substitute into the continuity equation $v_{2,3}$, $v_{2,4}$, ..., $v_{2,N-2}$

(5) March in the stream-wise direction up to i=M row; repeating steps (1) through (4).

(6) If transient calculations is desired, set the time step, and calculate the transient forcing functions; repeating steps (1) through (5).

It is noted that, the time-differencing scheme is fully implicit, and therefore, the time step is governed by the numerical accuracy considerations rather than numerical stability constraints.

TWIST is capable of calculating a sequence of steady state conditions or a steady-state leading into a transient condition.[9]

RESULTS AND COMPARISON WITH EXPERIMENTAL DATA

The TWIST code, briefly described in the previous section, is now used to simulate the steady state,[12] and transient[13] heat transfer tests performed at the Westinghouse Blanket Test Model.

The Westinghouse Blanket Test Model is a one-to-one scale model of a typical LMFBR 61-pin blanket assembly. The power level, axial and radial power distributions of the assembly are simulated using electrically heated fuel rod simulators.

The test section shown schematically in Fig. 2 is vertically mounted, with sodium entering at the bottom and flowing upward through the heated rod bundle, discharging from the duct near the vessel exit nozzle. The space outside the duct contains stagnant sodium and is compartmentalized by numerous horizontal and radial baffles to minimize heat loss by convective transfer in the annular space between the duct and the vessel walls.[12,13]

Parameters which can have significant effects on calculated temperature distributions include, inlet velocity distribution, bundle tolerance and especially the bundle bowing, pin distortion and the bundle housing thermo-mechanical behavior caused by heating effects.

In the present application the effect of bundle bowing and distortion are not taken into account. However, these effects can readily be included through adjustments in the hydraulic diameters and the porosity to match the experimental data.

In a typical fuel and blanket assembly, the flow area of the channels in the wall region is nearly twice as large as the flow area of the interior channels. As a result, the coolant temperature rise in the wall region is lower than in the interior channels. The wall channels act as a heat sink to the interior regions of the assembly. At low Reynolds numbers (or at low Peclet number; Pe=Re Pr), the flattening of the transverse temperature profile occurs as a result of the two distinct processes,[2,8] namely; first, by energy transport due to increased conduction, combined with wire wrap induced mixing, and secondly, by buoyancy-induced flow redistribution. As the wall channels are cooler than the interior channels, there will be density differences between the wall and the interior regions of the bundle, even in the absence of radial power skew. The effect of higher density, and to a lesser extent the higher viscosity in the wall region compared to the interior region, results in higher frictional forces in the wall channels. The combined effect of frictional and static head forces results in a net diversion of flow from the wall to the interior regions of the bundle. This buoyancy-induced cross flow tends to further flatten the transverse temperature gradient. This cross flow effect can be further enhanced in the presence of radial power skew across the bundle.[2,14]

The following analysis of simulation experiments demonstrates the importance of intra-subassembly processes as they influence the

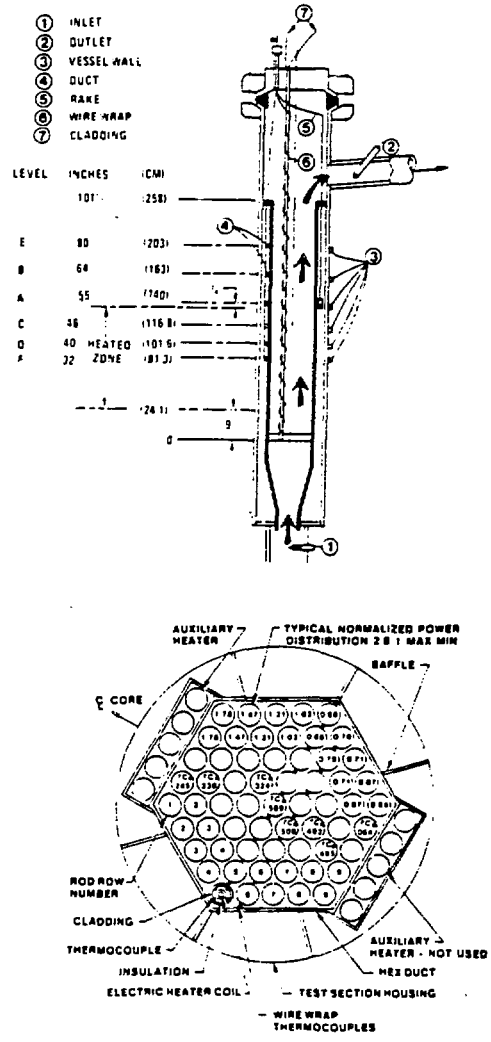

Figure 2 Schematics of the Westinghouse Blanket Test Section

steady state and transient sodium temperatures during forced, mixed, and free convection conditions.

The subassembly is divided into 40 radial and 20 axial nodes; with the heated region being represented by a chopped cosine axial power distribution, with peak to average of 1.4 as simulated in the experiments.[12]

Steady State

Figure 3 illustrates the calculated and measured[12] transverse temperature distribution corresponding to 2.8:1 power skew across the subassembly. It is seen that the agreement between the calculated and measured data improves as the heat transfer regime changes from forced to free convection.

The larger discrepancy in the low-power side of the bundle is influenced by the reduction in the flow area caused by fuel pin distortion and bowing as a result of large transverse power gradient. Similar observations have been made using the COTEC, ENERGY, and COBRA-IV computer codes.[14] Figure 3 also shows the transverse temperature profile corresponding to the midplane of the heated section. The better agreement between the TWIST and experimental data suggest that, the differential bowing seems to be more pronounced towards the top of the pin bundle.

Figure 3 also demonstrates the influence of the mixing parameter ϵ_∞^* on the bundle temperature profile. It is seen that a reduction in turbulent mixing reduces the cross-assembly temperature flattening at high Reynolds number leading to higher temperatures in the interior region and subsequently lower sodium temperatures in the side (wall) region.

Figure 4 shows the comparison between TWIST results and the measured longitudinal temperature distribution at Reynolds number of 7900. The agreement is good in the heated section, with predictions of peak temperature becoming more conservative near the subassembly outlet, where at high Reynolds numbers, mixing appears to be much stronger than calculated, thus leading to flatter measured transverse profile.

Transient

The Westinghouse transient experiments were performed by first establishing steady state conditions (power input, flow, temperature) and then decreasing the power input and sodium flow at pre-program rates.[13] The test series includes tests with heat input to all rods, and also to four rows (26 rods) only. The transients simulated both undercooling and overcooling events.

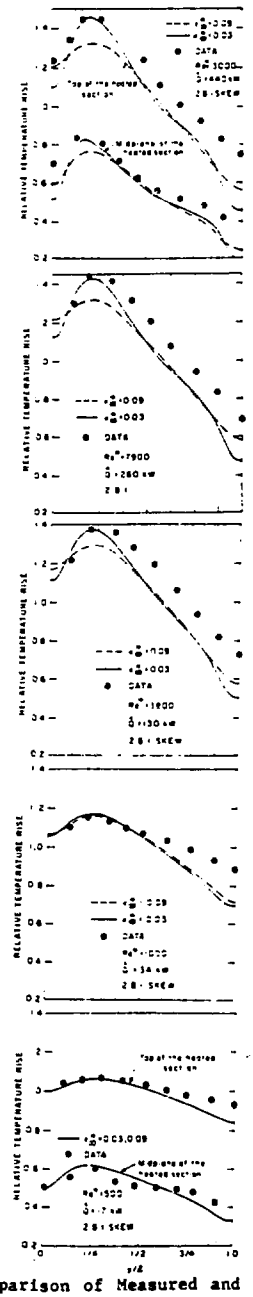

Figure 3 Comparison of Measured and Calculated Cross-Assembly Steady State Temperature Distributions

For the purpose of current simulation Test Run 613 is chosen. This test corresponds to 1:0 maximum-to-minimum heat input, where only 26 of the 61 rods were uniformly heated giving rise to large temperature gradients between the heated and unheated halves of the test section of Fig. 1.

Initially, the bundle was operating at 188 kw power, 56 gpm flow and 588K sodium inlet temperature condition. The bundle power and sodium flow rates are changed in a pre-programmed manner to achieve the desired rates.

In steady state operations, the power-to-flow ratio is a measure of the mean sodium temperature rise through the test section (see Fig. 5). During the transient, the temperature rise is also affected by the stored heat released from the heater rods and/or the duct walls. It must be noted that at present, TWIST assumes the heat input to be directly deposited into the coolant, and thus neglects the heat storage effects which can influence the early stages of the transient. However, modification of the code to include fuel pin to coolant heat transfer is straightforward.

Figure 6 illustrates the effect of transient operation on cross-assembly temperature profiles. Also shown are the corresponding measured values.

It is seen that a significant profile flattening takes place, similar to the steady state cases studied earlier. Furthermore, maximum discrepancies between the calculated and measured temperatures occur in the unheated side of the bundle, similar to the earlier steady state observations. However, the peak sodium temperatures are in excellent agreement with the test data.

Figure 7 shows that, peak sodium temperatures are in excellent agreement with the measured data where the temperatures follow the behavior of the power to flow ratio (Fig. 9). However, the peak temperatures are higher during the initial high flow part of the transient even when the power-to-flow ratio peaked back to near initial high values later in the transient. This reflects contribution of buoyancy-induced flow redistribution and transverse thermal conduction effects similar to those observed in low flow steady state tests. Heat transfer to the surrounding sodium and structures is also a significant contributing effect.

SUMMARY AND CONCLUSIONS

A two-dimensional porous-body model for Study of Steady state and transient Intra-subassembly thermal hydraulics, leading to a very fast running computer code was presented.

The code was then used to simulate steady state and transient sodium experiments performed at Westinghouse, where generally, good agreements were observed.

Numerical results supported by experimental data indicate that,

1) The [illegible], efficient marching technique employed by TWIST is adequate for study of forced, mixed, and free convection conditions in LMFBR subassemblies.

2) Significant cross-assembly temperature flattening takes place as a result of buoyancy-induced intra-subassembly flow redistribution, transverse thermal conduction and mixing.

3) The numerical efficiency (5 to 10 times faster than real time) and physical accuracy of this model, provides an efficient tool for study of long duration natural circulation transient in LMFBR assemblies.

Finally, it is planned to incorporate the TWIST code into the SSC[15] system-wide transient code for a complete and detailed simulation of protected transients in LMFBRs.

REFERENCES

1. M. Khatib-Rahbar and K. B. Cady, "Dynamical Models and Numerical Simulation of System-Wide Transients in Loop-Type LMFBRs," Nucl. Eng. and Design, 64, 259-281, (1981).

2. E. U. Khan, "LMFBR In-Core Thermal-Hydraulics: The State of the Art and U.S. Research and Development Needs," Pacific Northwest Laboratory, PNL-3337/UC-32, (April 1980).

3. E. U. Khan, W. M. Rohsenow, A. A. Sonin, and N. E. Todreas, "Manual for ENERGY I, II, III Computer Programs," Massachusetts Institute of Technology, Report COO-2245-18TR, (May 1975).

4. C. L. Wheeler, et al., "COBRA-IV-I: An Interim Version of COBRA for Thermal-Hydraulic Analysis of Rod Bundle Nuclear Fuel Element and Cores," Pacific Northwest Laboratory, BNWL-1962, (March 1976).

5. T. L. George, et al., "COBVRA-WC: A Version of COBRA for Single-Phase Multi-assembly Thermal-Hydraulic Transient Analysis," Pacific Northwest Laboratory, PNL-3259 (1980). Also see AICHE Symposium Series, No. 199, Vol. 76, 205-214.

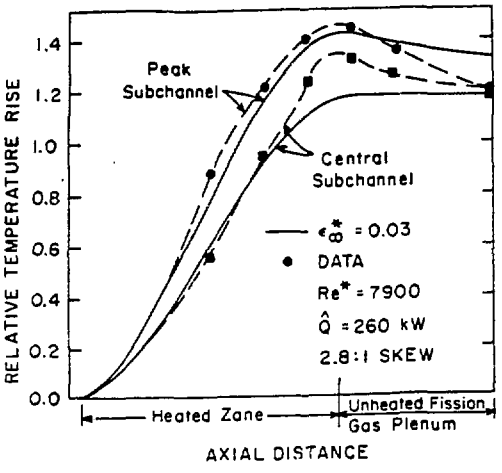

Figure 4 Comparison of Measured and Calculated Steady State Axial Temperature Distributions

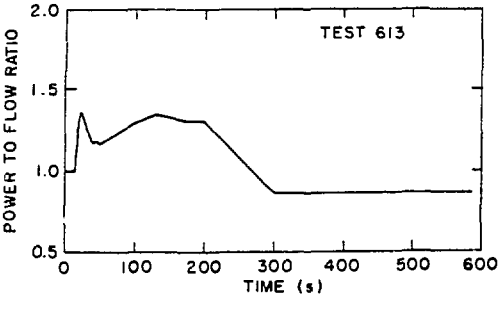

Figure 5 Transient Power-to-Flow Ratio (Forcing Function)

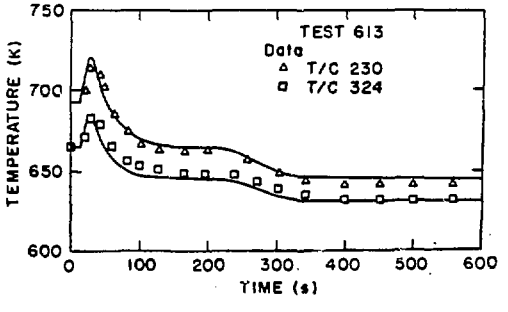

Figure 7 Comparison of Temporal Variation of Sodium Temperatures for T/C 230 & 324

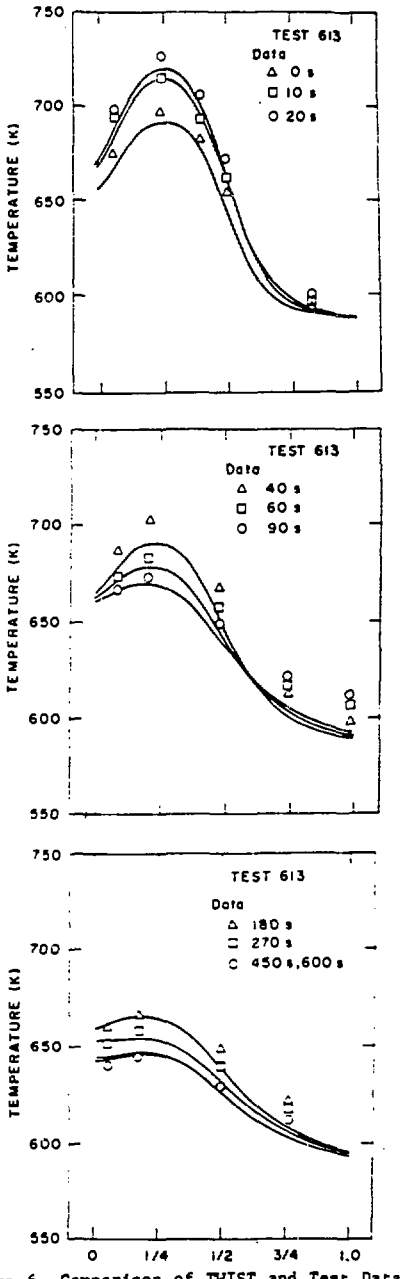

Figure 6 Comparison of TWIST and Test Data for Cross-Assembly Transient Temperature Distributions

6. W. L. Chen, M. A. Grolmes, and M. Ishii, "A Simple Forced Diversion Model for Study of Thermal-Hydraulic Transients in LMFBR Subassembly," Nucl. Eng. and Design, 45, 53-66 (1978).

7. H. G. Johnson, "CORA - A Computer Code for Thermal and Hydraulic Coupling of Reactor Core Assemblies," Hanford Engineering Development Laboratory, TC-1505, (September 1979).

8. M. Khatib-Rahbar and E. G. Cazzoli, "Intra-Assembly Flow Redistribution in LMFBRs: A Simple Computational Approach," Trans. Am. Nucl. Soc., 45, 816, (1983). Also see First Proceeding of Nuclear Thermal Hydraulics, 13, (1983).

9. M. Khatib-Rahbar and E. G. Cazzoli, "Two-Dimensional Modeling of Intra-Subassembly Heat Transfer and Buoyancy-Induced Flow Redistribution in LMFBRs," NUREG/CR-3498, (1984).

10. S. B. Patankar, Numerical Heat Transfer and Fluid Flow, Hemisphere Publishing Co., McGraw-Hill, New York, (1980).

11. R. W. Hornbeck, Numerical Marching Techniques for Fluid Flows With Heat Transfer, National Aeronautics and Space Administration, NASA-SP-297, Washington, D. C., (1973).

12. F. C. Engel, B. Minushkin, R. J. Atkins, and R. A. Markley, "Characterization of Heat Transfer and Temperature Distributions in an Electrically Heated Model of an LMFBR Blanket Assembly," Nucl. Eng. and Design, 62, 335-347, (1980).

13. F. C. Engel, R. A. Markley, and B. Minushkin, "Loss of Flow Transient Heat Transfer Tests of a Full Size LMFBR Blanket Model," ASME Paper No. 82-WA/HT-35, (1982).

14. J. Juneau and E. U. Khan, "Analysis of Steady-State Combined Forced and Free Convection Data in Rod Bundles," Argonne National Laboratory, FRA-TM-116, (January 1979).

15. J. G. Guppy, et al., "An Advanced Thermohydraulic Simulation Code for Transients in LMFBRs, SSC, Rev. 0," Brookhaven National Laboratory Report, BNL-NUREG-51650, (April 1983).

DISCLAIMER

This report was prepared as an account of work sponsored by an agency of the United States Government. Neither the United States Government nor any agency thereof, nor any of their employees, makes any warranty, express or implied, or assumes any legal liability or responsibility for the accuracy, completeness, or usefulness of any information, apparatus, product, or process disclosed, or represents that its use would not infringe privately owned rights. Reference herein to any specific commercial product, process, or service by trade name, trademark, manufacturer, or otherwise does not necessarily constitute or imply its endorsement, recommendation, or favoring by the United States Government or any agency thereof. The views and opinions of authors expressed herein do not necessarily state or reflect those of the United States Government or any agency thereof.